

## Comparative pathogenicity of goose parvovirus across different epidemic lineages in ducklings and goslings

Xiaolong Lu<sup>a,b,c,\*</sup>, Qianqian Xu<sup>a,\*</sup>, Miao Cai<sup>a</sup>, Meiqi Li<sup>a</sup>, Xiaoquan Wang<sup>a,b,c</sup>, Yanhong Wang<sup>a</sup>, Wenhao Yang<sup>a,b,c</sup>, Kaituo Liu<sup>b,c,d</sup>, Ruyi Gao<sup>a,b,c</sup>, Yu Chen<sup>a,b,c</sup>, Jiao Hu<sup>a,b,c</sup>, Min Gu<sup>a,b,c</sup>, Shunlin Hu<sup>a,b,c</sup>, Xiufan Liu<sup>a,b,c</sup>, and Xiaowen Liu<sup>a,b,c</sup>

<sup>a</sup>Key Laboratory of Avian Bioproducts Development, Ministry of Agriculture and Rural Affairs, Yangzhou University, Yangzhou, China;

<sup>b</sup>Jiangsu Co-Innovation Center for Prevention and Control of Important Animal Infectious Diseases and Zoonosis, Yangzhou University,

Yangzhou, China; <sup>c</sup>Jiangsu Key Laboratory of Zoonosis, Yangzhou University, Yangzhou, China; <sup>d</sup>Joint International Research Laboratory of Agriculture and Agri-Product Safety of Ministry of Education of China, Yangzhou University, Yangzhou, China

### ABSTRACT

The endemic status of goose parvovirus (GPV) continues to devastate the poultry industry in China. Novel GPV (NGPV) and Mutated GPV (MGPV) represent the predominant lineages. However, the comparative pathogenicity between these viruses remains poorly understood. Herein, we selected representative NGPV and MGPV strains as model viruses to assess their pathogenic potential both *in vitro* and *in vivo*. *In vitro* cellular and embryo assays demonstrated that both NGPV and MGPV were capable of replicating in DEF and GEF cells, leading to pronounced cytopathic effects. However, these viruses exhibited distinct levels of intra-embryonic replication capabilities. Furthermore, we conducted *in vivo* infection experiments and systematically evaluated the pathogenic differences between NGPV and MGPV by examining various indicators, including growth, clinical signs, gross pathology, skeletal development, viral load, and humoral response in the infected animals. The results showed that both NGPV and MGPV inhibited weight gain in goslings and ducklings, with NGPV exerting a more significant suppressive impact. MGPV induced classical gosling plague pathology in goslings, while NGPV led to short beak and dwarfism syndrome in ducklings, notably disrupting skeletal development. Moreover, MGPV and NGPV exhibited diverse host tropisms, with MGPV being more pathogenic to goslings and NGPV to ducklings. Both viruses elicited specific antibody responses, with MGPV being more effective in goslings and NGPV in ducklings. Additionally, MGPV exhibited stronger humoral response compared to NGPV. These findings enhance our understanding of the pathogenicity of prevalent GPV strains in waterfowl, offering a critical theoretical foundation for devising strategies to prevent GPV infections.

### ARTICLE HISTORY

Received 23 September 2024

Revised 22 January 2025

Accepted 21 April 2025

### KEYWORDS

NGPV; MGPV; pathogenicity; duckling; gosling


## Introduction

China emerges as a pre-eminent global producer of waterfowl, commanding over half of the worldwide production. Notably, the nation's dominance in goose farming is particularly noteworthy, occupying a substantial fraction of the international market [1]. Viral infections pose a significant threat to goose health, resulting in elevated mortality rates and diminished breeding productivity [2]. Goose plague, a prevalent disease among waterfowl, is caused by the goose parvovirus (GPV) [3]. GPV is a member of the Dependoparvovirus genus within the Parvoviridae family. Its genome is composed of single-stranded DNA (ssDNA), typically spanning around 5,000 to 5,200 nucleotides in length [4,5]. The gene-coding segment of this virus is divided into three structural proteins (named VP1, VP2,

and VP3) and two non-structural proteins (named NS1 and NS2). The three structural proteins are critical in the assembly of the viral capsid and are instrumental in the viral capability to infect host cells; the two non-structural proteins are crucial for the initial phases of GPV replication and for regulating [6,7]. GPV has the capacity to infect both goslings and ducklings, eliciting marked clinical manifestations [8,9]. The mortality rate is inversely correlated with the age of the infected birds, with younger birds being more vulnerable to its fatal impact [10]. Acute cases typically exhibit the hallmark symptoms of gosling plague, such as mucosal necrosis and intestinal embolisms, in addition to extensive hemorrhaging across various organs [11]. In contrast, older birds may exhibit a degree of resistance to gosling plague [12].

**CONTACT** Xiaowen Liu  [xwliu@yzu.edu.cn](mailto:xwliu@yzu.edu.cn); Xiufan Liu  [xfliu@yzu.edu.cn](mailto:xfliu@yzu.edu.cn)

\*Xiaolong Lu and Qianqian Xu contributed equally.

 Supplemental data for this article can be accessed online at <https://doi.org/10.1080/21505594.2025.2497904>

© 2025 The Author(s). Published by Informa UK Limited, trading as Taylor & Francis Group.

This is an Open Access article distributed under the terms of the Creative Commons Attribution-NonCommercial License (<http://creativecommons.org/licenses/by-nc/4.0/>), which permits unrestricted non-commercial use, distribution, and reproduction in any medium, provided the original work is properly cited. The terms on which this article has been published allow the posting of the Accepted Manuscript in a repository by the author(s) or with their consent.

GPV has diverged into several predominant clades, namely Novel GPV (NGPV), Mutated GPV (MGPV), Attenuated GPV, and Early GPV [13]. In recent years, NGPV and MGPV strains are the most prevalent in circulation. Duck-originating strains predominantly fall within the NGPV lineage, while the MGPV lineage is largely composed of isolates from geese [14,15]. NGPV preferentially infects ducklings, with short beak and dwarfism syndrome (SBDS) as the primary outcome [16]. This condition is characterized by beak abnormality, tongue protrusion, and systemic skeletal deformities, including brittle bones and a heightened risk of fractures [17,18]. Conversely, the pathogenicity of MGPV strains remains a less understood area in scientific research.

This investigation selected representative NGPV and MGPV strains as model viruses to evaluate their *in vitro* and *in vivo* pathogenicity. A comparative *in vitro* study was performed to assess the cellular lesions and intra-embryonic proliferation abilities of NGPV and MGPV. Furthermore, a comparative *in vivo* study was conducted to assess the pathogenic potential of NGPV and MGPV in goslings and ducklings, respectively. To quantify the inhibitory effects of NGPV on bone development in ducklings, various imaging techniques were employed, including X-ray, microcomputed tomography (Micro-CT), and histological analysis of bone sections. The evaluation was both qualitative and quantitative to delineate the effects on skeletal growth. The findings enhance our understanding of the pathogenic impact of prevalent GPV strains on waterfowl. As such, these results provide a critical theoretical basis for devising strategies to prevent and manage GPV infections.

## Materials and methods

### Ethics statement

All animal experiments were conducted in strict accordance with the guidelines outlined in the Guide for the Care and Use of Laboratory Animals by the Ministry of Science and Technology of the People's Republic of China. The Administrative Committee for Laboratory Animals of Yangzhou University affiliated with Jiangsu Province (Permission number: 202302083) approved all of the animal studies according to the guidelines of Jiangsu Laboratory Animal Welfare and Ethical of Jiangsu Administrative Committee of Laboratory Animals.

### Viruses, animals, embryos, and cells

The NGPV strain Duck/China/X6/2021 and the MGPV strain Goose/China/GS2211102/2022 were

obtained from our laboratory stocks. 1-day-old non-immunized goslings and Cherry Valley ducklings were purchased from farms in Yangzhou and Taizhou, respectively. The ducklings and goslings were tested for antibody levels in their serum using a 450 nm wavelength ( $OD_{450}$ ) measurement. If they had GPV antibodies, further challenge tests would be skipped, and future test animals must be free of GPV antibodies. Non-immunized goose and duck embryos were sourced from farms in Yangzhou and Taizhou, respectively. These embryos were incubated in our laboratory until they were 9 days old. Goose embryo fibroblasts (GEF) and duck embryo fibroblasts (DEF) were then isolated from the respective goose and duck embryos.

### Cytopathic observation

Cytopathic effects (CPE), such as cell shrinkage, debris formation, and increased cellular translucency, were monitored using a cellular morphology assay under microscopy. Specifically, GEF or DEF cells seeded in 6-well plates were either mock-infected or exposed to 1 mL of virus solution. Notably, MGPV and NGPV were cultured in DEF and GEF cells, respectively, with each passage lasting 120 hours. CPE were assessed following the first and fifth viral passages. The cellular morphology of each treatment group was examined at the first and fifth viral passages. The PBS group acted as a negative control, while morphological changes in the infected group indicated cellular damage.

### Determination of intra-embryonic growth curve

The GPV strains were inoculated into the allantoic cavities of susceptible embryos, with five replicates for each strain. The MGPV strain was introduced into 9-day-old goose embryos, while the NGPV strain was administered to 9-day-old duck embryos. Allantoic fluid samples (200  $\mu$ L) were collected from each surviving embryo at 72, 96, 120, 144, 168, and 192 hours post-inoculation (hpi). The sampled fluid was processed with the EasyPure® Viral DNA/RNA Kit for DNA extraction. DNA quantification was carried out using TaqMan probe-based quantitative PCR. Replication kinetics were plotted using GraphPad Prism 8.0 software.

### Animal experimental design and clinical lesion detection

The GPV strains were serially diluted 10-fold in sterile PBS, with dilutions from  $10^{-3}$  to  $10^{-8}$ . The diluted

samples were injected into the allantoic cavities of 9-day-old gosling and duck embryos, with 0.2 mL given to five embryos per dilution. The allantoic fluid was sampled from each embryo at 168 h, and DNA was extracted using the EasyPure® Viral DNA/RNA Kit according to the instructions. DNA quantification was conducted via TaqMan probe-based quantitative PCR, and the EID<sub>50</sub> was determined using the Reed-Muench method. Subsequently, both virus strains were injected intramuscularly into the leg muscles of 1-day-old goslings and ducklings at a dose of  $10^{5.5}$  EID<sub>50</sub>/0.2 mL, with 20 animals per strain. Simultaneously, a control group of 20 1-day-old goslings and ducklings received an equivalent volume of PBS. 60 goslings and 60 ducklings were used separately in this study. The animals were observed for clinical signs and organ lesions at specified time intervals. Animals in each group were kept in separate rooms to prevent mixed infections during experiments. Animals and their organs in the infected group, unlike the PBS group, exhibited abnormal changes indicative of classic clinical and pathological symptoms. The sample size of this study was determined based on published research on GPV pathogenicity [13].

### **Skeletal development detection**

After the viral challenge experiments outlined above, a random subset of five animals from each group was selected and tagged. Morphometric and body weight measurements were performed at 1, 4, 7, 14, 21, and 28 days post-inoculation (dpi) for these animals. The collected data were then analyzed to plot trend curves for body weight, beak length, and beak width using GraphPad Prism 8.0 software. Body weight was monitored from 1 dpi, with the weight on 1 dpi established as 100%. Beak length and width were monitored from 1 dpi, using the 1 dpi measurements as the baseline (100%). Significant changes in body weight, beak length, and beak width in the infected group, compared to the PBS group, indicated abnormal development. Additionally, at 28 dpi, three random ducklings from the NGPV-infected and PBS control groups were chosen for comprehensive X-ray imaging of the entire left leg. The tibial tissue from the right leg was carefully dissected, removing feathers, skin, muscles, blood vessels, and connective tissues to maintain its structure. The excised tibias were then fixed in 4% paraformaldehyde for Micro-CT scanning and subsequent sectioning. HE staining assesses the formation of a well-defined, intact marrow cavity. Masson staining differentiates mature (red) from new (blue) bone collagen. Tartrate-resistant acid phosphatase staining highlights

osteoclasts in red via marker enzymes. All imaging, scanning, and histological processing were conducted at Wuhan Bailaibo Technology Co., Ltd.

### **Viral load quantification**

Post-viral challenge, three unmarked animals per group were randomly chosen for humane euthanasia at 1, 7, 14, 21, and 28 dpi. The experimental population comprised a total of 45 goslings and 45 ducklings. Tissue samples (0.3 g) from the heart, liver, spleen, lungs, kidneys, and intestines were aseptically harvested from each animal. These samples were processed with three times their volume of double antibody PBS, subjected to three freeze-thaw cycles, and then homogenized. After centrifugation at 8000 r/min for 5 min, supernatants were carefully collected, divided into aliquots, and stored at  $-70^{\circ}\text{C}$  for subsequent analysis. Nucleic acids were extracted using the EasyPure® Viral DNA/RNA Kit as per the manufacturer's instructions. DNA presence in tissue samples across different animal groups, organs, and time points was assessed by TaqMan probe-based qPCR. Virus replication dynamics in individual organs were visualized using GraphPad Prism 8.0 software.

### **Antibody level determination**

Post-viral challenge, 1 mL of blood was collected from each three random animal euthanized at 1, 7, 14, 21, and 28 dpi. The experimental population comprised a total of 45 goslings and 45 ducklings. The samples were incubated at  $37^{\circ}\text{C}$  for one hour, followed by serum separation of the supernatant, which was then stored at  $-20^{\circ}\text{C}$  for later analysis [19]. Serum antibody titers were measured using an indirect ELISA. In this assay, a purified GPV antigen was coated at a concentration of 0.25 ng/ $\mu\text{L}$ , and serum was diluted 1:500. The optical density at 450 nm (OD<sub>450</sub>) was measured to quantify antibody levels. In the ELISA assay, a *P/N* ratio of  $\geq 2.1$  is indicative of a positive result; otherwise, it is considered negative.

### **Statistical analysis**

The data are presented as the means  $\pm$  standard deviations of three independent replicates derived from a representative experiment. Statistical significance was assessed using either t-test or two-way analysis of variance (ANOVA), with *P-value*  $< 0.05$  denoting significance. In the figure, (\*), (\*\*), (\*\*\*), and (\*\*\*\*) indicate *P*-values  $< 0.05$ ,  $< 0.01$ ,  $< 0.001$ , and  $< 0.0001$ . All statistical evaluations were performed using GraphPad Prism 8.0 software.

## Results

### ***MGPV and NGPV induced significant cellular lesions***

NGPV and MGPV were cultured in DEF and GEF cells, respectively, with each passage lasting 120 hours. To evaluate the cytopathic effects of NGPV and MGPV, the first and fifth passages were examined for their cytotoxicity on host cells. Control cells maintained their fibrous morphology with minimal rounding or rupture. In contrast, both viruses induced cytopathic effects (CPE) in DEF and GEF cells, manifesting as cell shrinkage, membrane lysis, debris formation, and increased cellular translucency. NGPV induced CPE in DEF cells across both passages, with the fifth passage showing a more severe response in GEF cells. Similarly, MGPV-infected GEF and DEF cells displayed significant CPE, with the fifth passage exhibiting a more pronounced effect than the first (Figure 1a). These results indicate that both MGPV and NGPV can replicate in DEF and GEF cells, resulting in marked CPE.

### ***MGPV and NGPV exhibited differential intra-embryonic proliferation abilities***

To evaluate the replication kinetics of MGPV and NGPV in embryos, the viruses were inoculated into respective host embryos and incubated for defined periods. Subsequently, allantoic fluid was sampled and analyzed using TaqMan probe-based qPCR to quantify the virus. The results revealed an overall upward trend in viral copy number throughout the infection period, confirming the replication capabilities of MGPV and NGPV in goose and duck embryos, respectively. MGPV showed a consistent increase in copy number without reaching a peak, whereas NGPV peaked at 168 hpi before declining at 192 hpi (Figure 1b). These results highlight the distinct replication profiles of MGPV and NGPV in their respective host embryos.

### ***NGPV caused stronger weight suppression than MGPV in goslings and ducklings***

To evaluate the differences in pathogenicity of MGPV and NGPV *in vivo*, we further conducted systematic *in vivo* challenge experiments (Figure 2a). Body weight was monitored from 1 dpi, with the weight on 1 dpi established as 100%. Subsequent measurements were taken on 4, 7, 14, 21, and 28 dpi, expressed as a percentage of the weight on each respective day relative to the initial weight. Both infected and control animal groups exhibited increasing body weights, although the growth rates of infected groups were

slower than the controls. A significant divergence in weight gain was observed among duckling groups from 14 dpi onwards. The control group showed a substantially higher growth rate (averaging 900%, 1157%, and 1397%) than the infected groups, and the MGPV group had a significantly higher rate (averaging 335%, 470%, and 886%) than the NGPV group (averaging 710%, 893%, and 987%) at 14, 21, and 28dpi. These findings indicate that both NGPV and MGPV inhibit weight gain in ducklings, with NGPV having a more substantial inhibitory effect than MGPV. Additionally, the weight growth rate of goslings in the NGPV and MGPV groups was significantly lower than the PBS group after 21 dpi, particularly pronounced in the NGPV group (averaging 625% at 21 dpi and 789% at 28 dpi). Statistical significance in the MGPV group was only evident at 28 dpi (averaging 796%), potentially due to individual variation among goslings (Figure 2b). Thus, the findings suggest that both NGPV and MGPV suppress weight gain in goslings and ducklings, with NGPV demonstrating a more potent inhibitory impact.

### ***NGPV exerted a greater inhibitory effect on beak growth than MGPV in ducklings, but not in goslings***

Beak length and width were tracked from 1 dpi, with the initial measurements on 1 dpi serving as the baseline (100%). Subsequent measurements were taken on 4, 7, 14, 21, and 28 dpi, with each day's index or width expressed as a ratio of the N-day value to the 1-day value. The results revealed a general upward trend in beak length and width across all groups, although the growth rates in the infected groups were slower than in the control group. Variations in beak growth rates were observed among the different groups. Notably, significant differences in beak length and width growth rates were detected in ducklings, but not in goslings. The control group displayed higher beak growth rates compared to the infected groups. NGPV significantly inhibited beak development by 7 dpi, whereas MGPV's significant effect was observed at 21 dpi (Figure 2c,d). These findings suggest that both NGPV and MGPV significantly impede beak development in ducklings, with NGPV exerting a more pronounced inhibitory effect than MGPV, and with no significant impact observed in goslings.

### ***MGPV exhibited pathogenicity towards goslings, whereas NGPV was pathogenic to ducklings***

Goslings infected with MGPV and ducklings infected with NGPV displayed distinct clinical symptoms, while other groups showed minimal clinical signs. Specifically, MGPV-infected goslings presented noticeable symptoms



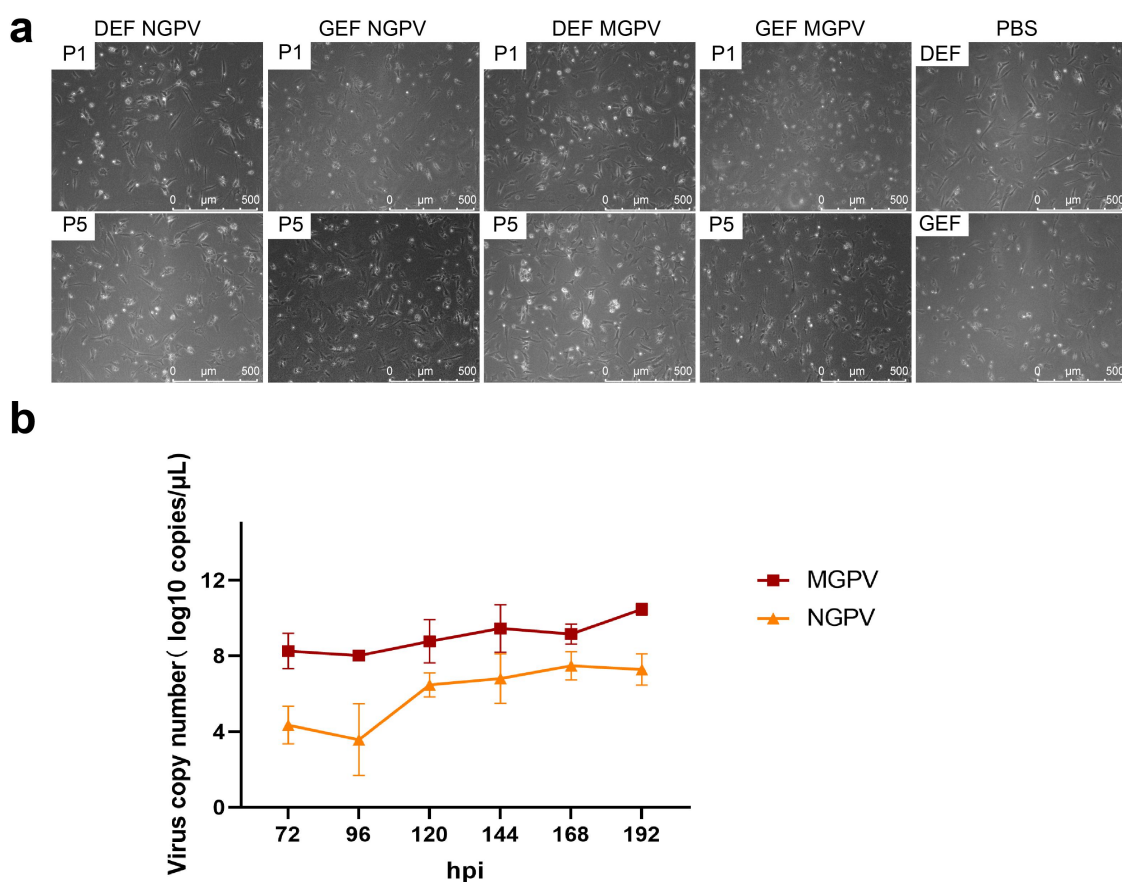


**Figure 1.** Cytopathic effect and replication curve of GPV in primary cells and embryos. (a) GEF or DEF cells in 6-well plates underwent mock infection or virus inoculation. MGPV and NGPV were cultured in DEF and GEF cells, respectively, with 120 h per passage. CPE from 1st and 5th passages was assessed under a microscope. Scale bar: 500 μm. (b) The MGPV strain was inoculated into 9-day-old gosling embryos, while the NGPV strain into duck embryos of the same age. Allantoic fluid was sampled from each viable embryo at 72, 96, 120, 144, 168, and 192 hpi, followed by DNA extraction, quantification, and replication curve generation using GraphPad prism 8.0.

from 3 dpi, including lethargy, inappetence, ataxia, a preference for recumbency, and ruffled plumage (Figure 3a). Post-mortem analyses of these infected goslings revealed significantly smaller heart, spleen, and liver compared to controls, with dark red hemorrhages in the myocardium and spleen. The liver appeared jaundiced, with extensive surface hemorrhages and intestinal necrosis (Figure 3b,c,d,e). Additionally, embolic mucosal tissue and dark purple renal congestion were noted, indicative of the classical pathology of gosling plague (Figure 3f). In contrast, NGPV-infected ducklings exhibited marked growth and developmental deficits, characterized by reduced size, an aversion to standing, and unresponsiveness to herding, and were notably smaller than control ducklings. Abnormal beak development was apparent, with significantly reduced length and width relative to control ducklings. Moreover, the tongue protruded abnormally from the beak (mark with a white box), a hallmark of the classic SBDS (Figure 3g).

### ***NGPV significantly impaired the skeletal development of ducklings***

NGPV-infected ducklings exhibited pronounced symptoms of SBDS at the previous study, prompting a comprehensive analysis to elucidate the specific effects of NGPV on duckling skeletal development. X-ray scans were conducted on the leg bones of NGPV-infected and control ducklings to assess skeletal growth (Figure 4a,b). The X-ray results revealed a significant suppression of skeletal development in NGPV-infected ducklings, with the lengths of the tibia (averaging 50.3 mm) and femur (averaging 28.5 mm) significantly shorter compared to those in the PBS-treated ducklings (averaging 84.4 mm of tibia and 50.3 mm of femur). Additionally, the metatarsal and toe bones in the PBS-treated ducklings were notably longer than those in the NGPV-infected ducklings. Reduced bone density enhances the penetration of X-rays through skeletal

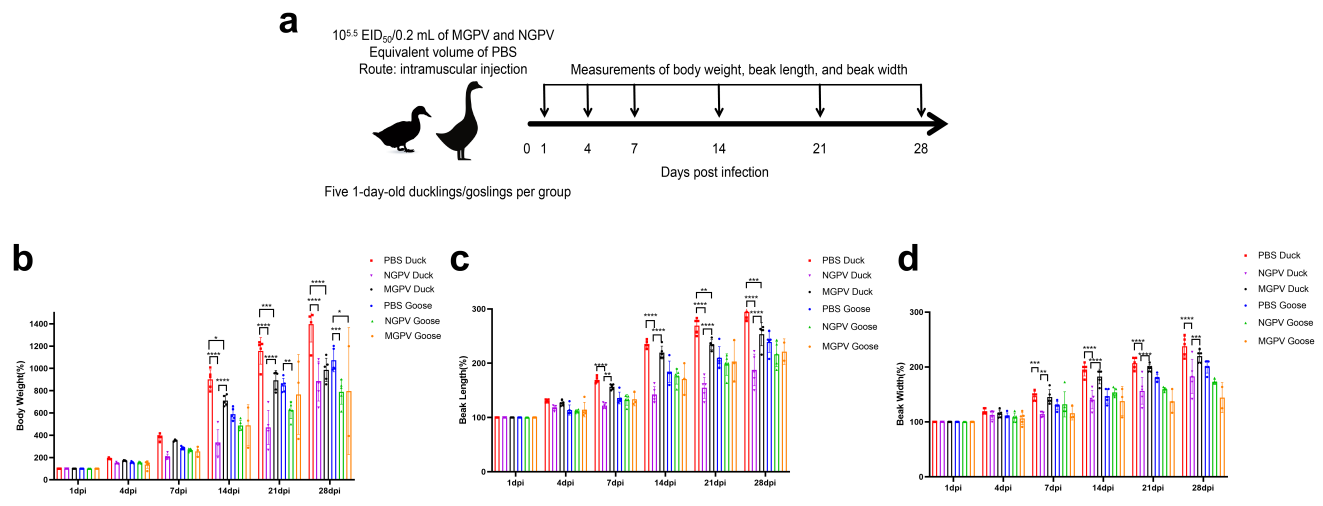


**Figure 2.** Growth and development of animals challenged by GPV. Curve of body weight of animals challenged by GPV. (a) MGPV and NGPV were intramuscularly inoculated at  $10^{5.5}$  EID<sub>50</sub>/0.2 mL into 1-day-old goslings and ducks, with PBS-inoculated controls. Five animals per group were randomly selected and monitored for morphometrics and weight at 1, 4, 7, 14, 21, 28 dpi. Data were analyzed for (b) weight, (c) beak length, and (d) width trends using GraphPad prism 8.0. The schematic representation is created with WPS software. \* $p < 0.05$ , \*\* $p < 0.01$ , \*\*\* $p < 0.001$ , \*\*\*\* $p < 0.0001$ .

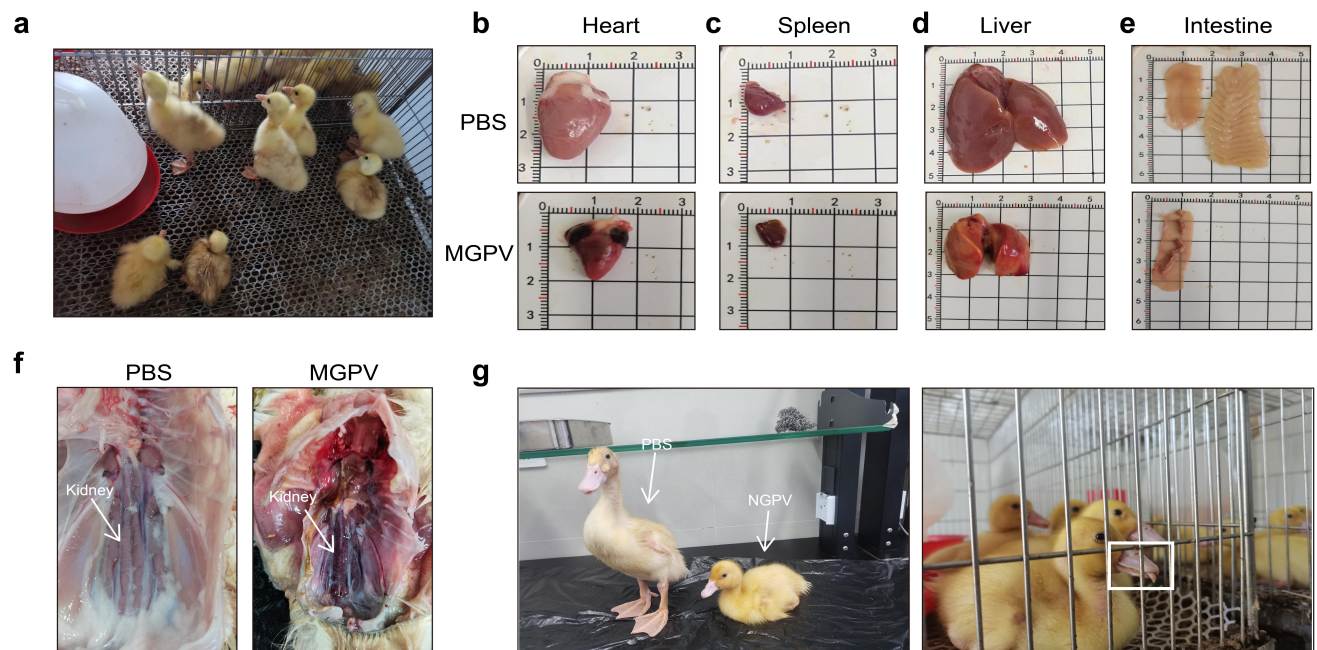


**Figure 3.** Clinical symptoms and pathological changes induced by GPV. (a) Clinical symptoms of MGPV- infected goslings. (b-f) pathological changes of heart, spleen, liver, intestine and kidney of MGPV- and mock-infected goslings. (g) Clinical symptoms of NGPV- infected goslings. The white box indicates a hallmark of the classic SBDS.

structures, leading to reduced radiographic brightness. Consequently, a comparative analysis of the grayscale values for the tibia and femur was performed between the two groups, revealing a significant discrepancy in grayscale values, indicating a decrease in osseous density in NGPV-infected ducklings (averaging 112.3 of tibia and 198.3 of femur) relative to the controls (averaging 170.0 of tibia and 248.3 of femur). Furthermore,

the bone cortex of NGPV-infected ducklings displayed a reduction in thickness and a narrowing of the medullary cavity compared to the control group (Figure 4c,d,e,f).

To elucidate the internal architecture of the tibias, micro-CT scanning and subsequent three-dimensional reconstruction were employed on tibias from ducklings in the NGPV-infected group and the control group

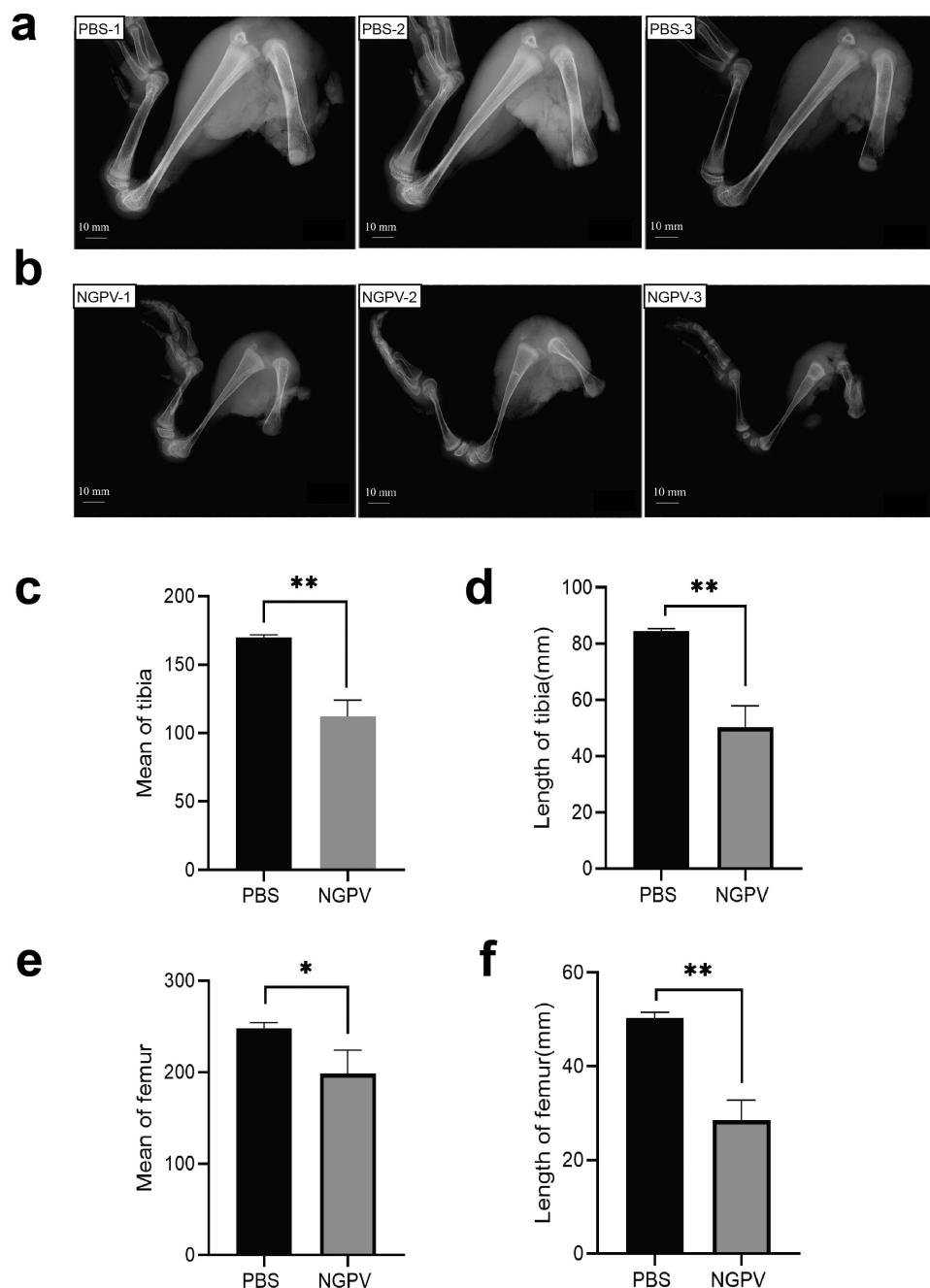


**Figure 4.** X-ray scanning results of bones of the ducklings infected with NGPV. Three ducklings each from the NGPV- and PBS-infected groups were selected for comprehensive X-ray imaging of bones. (a) The X-ray scanning results of the PBS-infected ducklings. (b) The X-ray scanning results of the NGPV-infected ducklings. Scale bar: 10 mm. (c) Mean of tibia of PBS- and NGPV-infected infected ducklings. (d) Length of tibia of PBS- and NGPV-infected infected ducklings. (e) Mean of femur of PBS- and NGPV-infected infected ducklings. (f) Mean of femur of PBS- and NGPV-infected infected ducklings. \* $p < 0.05$ , \*\* $p < 0.01$ .

(Figure 5a,b). Concurrently, a quantitative analysis was conducted to assess tibial structural parameters. The results indicated that the bone volume fraction (BV/TV) (averaging 10.8% of NGPV and 25.7% of control) and bone mineral density (BMD) (averaging 0.02 g/cm<sup>3</sup> of NGPV and 0.09 g/cm<sup>3</sup> of control) of the NGPV-

infected ducklings were significantly lower than those of the control ducklings, indicating a substantial loss of bone mass due to NGPV infection (Figure 5c,d). Additionally, the NGPV-infected group exhibited a decrease in trabecular bone number (Tb.N) (averaging 1.4 of NGPV and 0.8 of control), a reduction in

mean trabecular thickness (Tb.Th) (averaging 0.1 mm of NGPV and 0.2 mm of control), an increase in trabecular separation (Tb.Sp) (averaging 2.3 mm of NGPV and 0.8 mm of control), and an increase in structural model index (SMI) (averaging 1.4 of NGPV and 0.8 of control) compared to the control group (Figure 5e,f,g,

h). These alterations suggest a predominance of rod-like trabeculae and indicate that the quantity, morphology, and arrangement of trabeculae are integral to bone strength. Therefore, the findings suggest that NGPV can significantly decrease bone mass, density, and strength in ducklings compared to the control group.

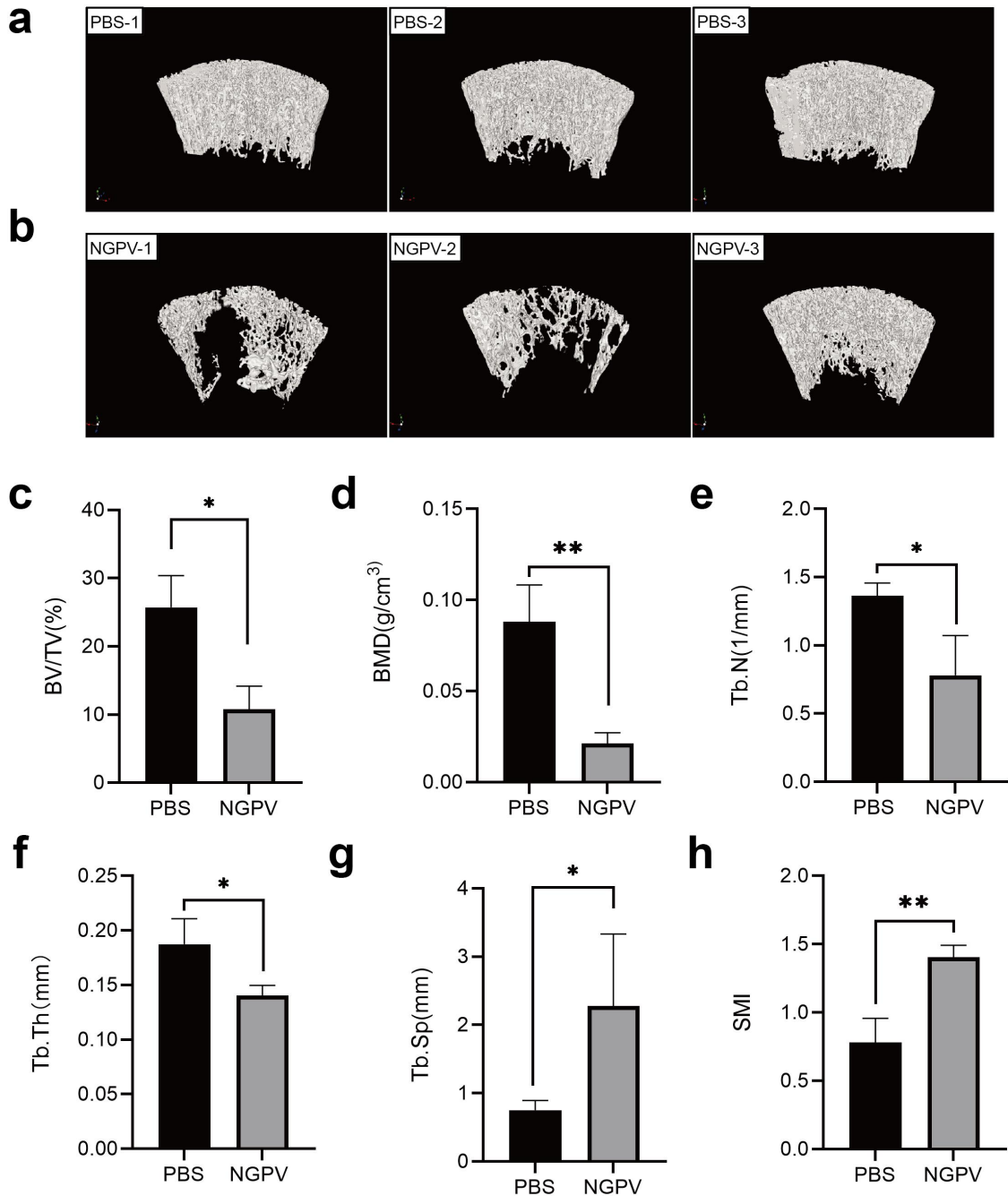


**Figure 5.** Micro-CT detection results of bones of the ducklings infected with NGPV. Three ducklings each from the NGPV- and PBS-infected groups were selected for comprehensive micro-CT scanning of bones. (a) The micro-CT scanning results of the PBS-infected ducklings. (b) The micro-CT scanning results of the NGPV-infected ducklings. (c) Bone volume analysis of PBS- and NGPV-infected infected ducklings. (d) Bone mineral density analysis of PBS- and NGPV-infected infected ducklings. (e) Number of bone trabeculae of PBS- and NGPV-infected infected ducklings. (f) Average thickness of bone trabeculae of PBS- and NGPV-infected infected ducklings. (g) Separation degree of bone trabeculae of PBS- and NGPV-infected infected ducklings. (h) Structure model index of PBS- and NGPV-infected infected ducklings. \* $p < 0.05$ , \*\* $p < 0.01$ .



This implies that NGPV contributes to predisposing infected ducklings to bone pathologies, including fractures, osteoporosis, and skeletal abnormalities.

### ***The multi-staining assays elucidated the crucial impact of NGPV on skeletal development of ducklings***

To visually assess skeletal development in ducklings, tissue sections from NGPV-infected and control group ducklings at 28 dpi were prepared and stained with HE, Masson, and Tartrate-resistant acid phosphatase (TRAP) stains. Endochondral ossification is the primary mode of bone formation in appendicular skeletal elements such as the tibia, involving the sequential replacement of pre-existing cartilage templates with bone tissue [20]. HE staining revealed that the skeletal morphology of ducklings in the control group was predominantly fully developed, with a clearly defined and structurally intact marrow cavity observed. Concurrently, the epiphyseal structure in the control group ducklings was well established, pertinent to the potential elongation of the tibia. The epiphyseal plate was instrumental in this process, exhibiting distinct quadrants when viewed from left to right: the cartilage reserve zone, cartilage hyperplasia zone, cartilage calcification zone, and osteogenic zone. Furthermore, the trabecular bone of the control group ducklings exhibited a regular arrangement of bone trabeculae with a broader morphology (Figure 6a). In contrast, bone development in NGPV-infected ducklings was delayed, remaining in the initial stages; the marrow cavity in the tibia was unformed, with the intertrabecular spaces serving as the provisional marrow cavity; the epiphyseal structure was underdeveloped, populated by an abundance of chondrocytes, leading to a denser cartilage matrix. Additionally, the trabecular bone in infected ducklings displayed a disorganized architecture with reduced thickness (Figure 6b). Therefore, HE staining results indicate that NGPV infection in ducklings results in suppressed bone development.

Masson staining is utilized to highlight collagen fibers within bone tissue, with mature bone collagen appearing red and newly formed bone collagen blue. In the control group, extensive areas of red-stained mature bone tissue were observed, whereas the NGPV-infected group showed blue staining (Figure 6c,d). TRAP staining targets osteoclast marker enzymes, giving osteoclasts a distinct red color. The TRAP staining results indicated that multinucleated osteoclasts were distributed around calcified cartilage and transitional trabeculae in both the NGPV-infected and control groups, indicating a balance between bone resorption and

formation. Compared to the control group, the NGPV-infected group displayed an increased osteoclast count, suggesting enhanced bone resorptive activity (Figure 6e,f). Therefore, the combined staining results suggest that NGPV infection can significantly impair duckling bone development.

### ***MGPV demonstrated a higher susceptibility in goslings, whereas NGPV showed a greater susceptibility in ducklings***

To evaluate the comparative replication of MGPV and NGPV in ducklings versus goslings, qPCR was utilized to quantify viral loads in various organs at specified time points. Although the replication efficiency of MGPV varied among different animal species due to individual differences, the virus retained the ability to replicate within these hosts. The results revealed that MGPV was present in multiple organs of both goslings and ducklings from 1 dpi, with particularly high titers in the liver and intestines. After MGPV infection, viral loads in both goslings and ducklings increased over time, reaching a peak at 7 and 14 dpi (averaging  $\geq 10^{6.6}$  copies/ $\mu$ L in goslings and  $\geq 10^{3.3}$  copies/ $\mu$ L in ducklings). Thereafter, viral loads in ducklings decreased, while those in goslings remained elevated. Significantly, viral loads of MGPV in goslings were consistently higher than in ducklings, with the most pronounced differences observed at 28 dpi (averaging  $\geq 10^{5.1}$  copies/ $\mu$ L in goslings and  $\geq 10^{2.2}$  copies/ $\mu$ L in ducklings) (Figure 7a,b,c,d,e). These results indicate that MGPV can replicate in both goslings and ducklings, with a greater replication capacity in goslings compared to ducklings.

In the NGPV-infected groups, the viral replication levels were generally higher in ducklings than in goslings. Specifically, the virus was detectable in all organs of infected ducklings at 1 dpi, whereas no viral presence was observed in infected goslings at the same time point, suggesting that NGPV exhibits a more potent infective capacity in ducklings than in goslings. At 7 dpi, the viral load in the liver and intestines of the ducklings was notably higher than in the gosling-infected group. The peak viral load was reached in both goslings (averaging  $\geq 10^{5.6}$  copies/ $\mu$ L) and ducklings (averaging  $\geq 10^{7.5}$  copies/ $\mu$ L) at 14 dpi. Subsequently, the viral load in ducklings remained high through 28 dpi (averaging  $\geq 10^{5.1}$  copies/ $\mu$ L), while in goslings, it showed a gradual decline (averaging  $\geq 10^{1.3}$  copies/ $\mu$ L) (Figure 7f,g,h,i,j). Thus, NGPV replicates earlier and more stably in ducklings than in goslings, indicating a higher susceptibility in ducklings.

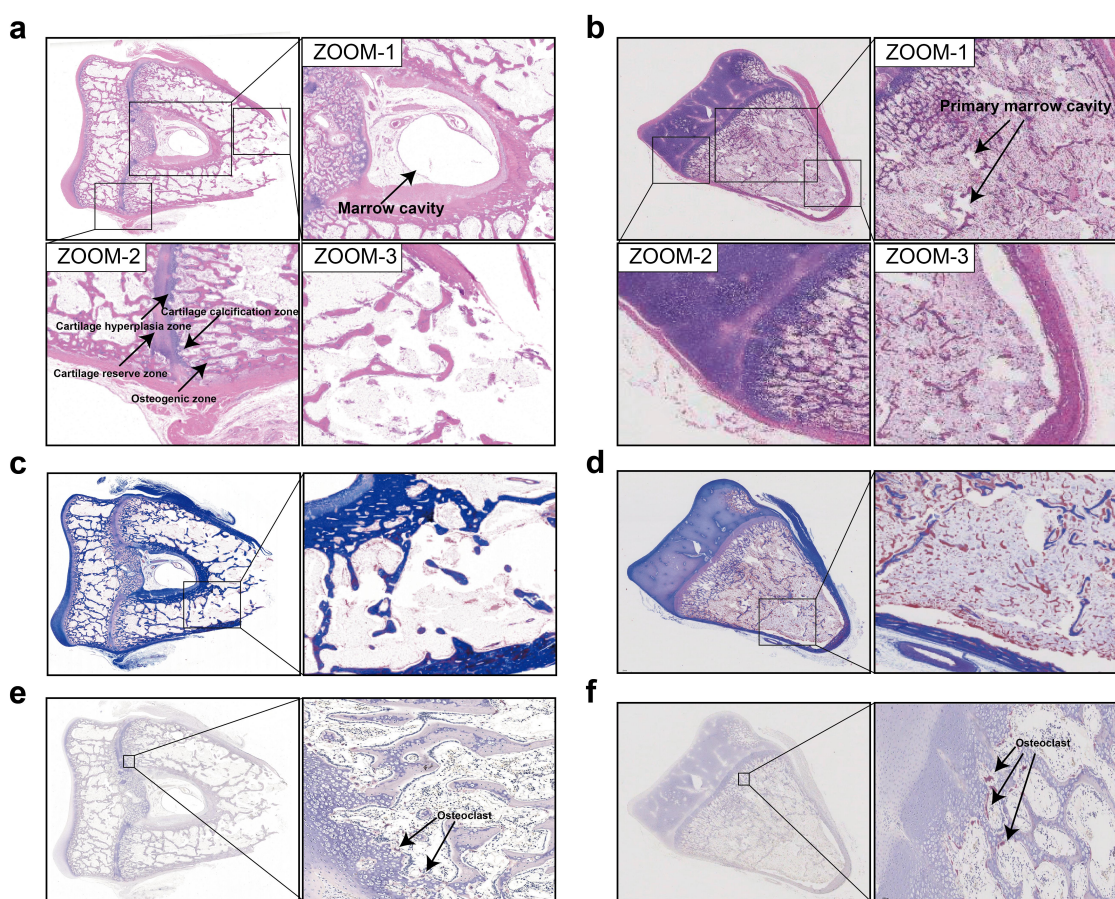


**Figure 6.** Bone staining analysis of ducklings infected with NGPV. Three ducklings each from the NGPV- and PBS-infected groups were selected for comprehensive bone sectioning. (a) HE staining of bone tissues of ducklings in PBS group, and the structure of skeletal is basically formed. ZOOM-1: the marrow cavity structure has been formed; ZOOM-2: the epiphysis is formed and four regions of the epiphysis are evident, including the cartilage reserve zone, cartilage hyperplasia zone, cartilage calcification zone, and osteogenic zone; ZOOM-3: the trabecular bones. (b) HE staining of bone tissues of ducklings in NGPV group. ZOOM-1: primary bone marrow cavity formed by the intertrabecular space; ZOOM-2: the epiphysis was not formed, numerous chondrocytes were present, and the cartilage matrix was thick; ZOOM-3: most of the bone trabeculae are transitional and arranged disorderly. (c) Masson staining of bone tissue of ducklings in PBS group, and the stained area was extensively red, representing mature bone tissue. (d) Masson staining of bone tissue of ducklings in NGPV group, and the stained area was extensively blue, representing immature bone tissue. (e) Trap staining of bone tissue of ducklings in PBS group, and the red arrow points to osteoclasts. (f) Trap staining of bone tissue of ducklings in NGPV group, and the red arrow points to osteoclasts.

### ***MGPV replicated more robustly in goslings than NGPV, with the opposite trend observed in ducklings***

To elucidate the differential replication capabilities of MGPV and NGPV within the same host, we conducted a comparative analysis of their replication levels in goslings and ducklings. In infected goslings, the viral copy number of MGPV consistently exceeded that of NGPV throughout the infection. The replication level of MGPV was significantly higher than that of NGPV at both the early (1 dpi) and late (21 and 28 dpi) stages of infection. At 1 dpi, MGPV replicated across multiple organs in goslings, whereas NGPV exhibited limited replication

confined to a minimal quantity in the spleen of a single goose, with a low viral titer of approximately  $10^{2.0}$  copies/ $\mu\text{L}$ . At 21 and 28 dpi, the viral copy number of MGPV was significantly higher than that of NGPV in various gosling organs, with MGPV copy numbers exceeding  $10^{5.0}$  copies/ $\mu\text{L}$ , in contrast to the lower copy numbers observed for NGPV (Figure 8a,b,c,d,e).

In infected ducklings, NGPV displayed a stronger replication capacity than MGPV. Both viruses replicated in various duckling organs throughout the infection period. MGPV showed a higher viral copy number at 1 dpi, with notable differences in the gut. Subsequently, NGPV surpassed MGPV in viral copy

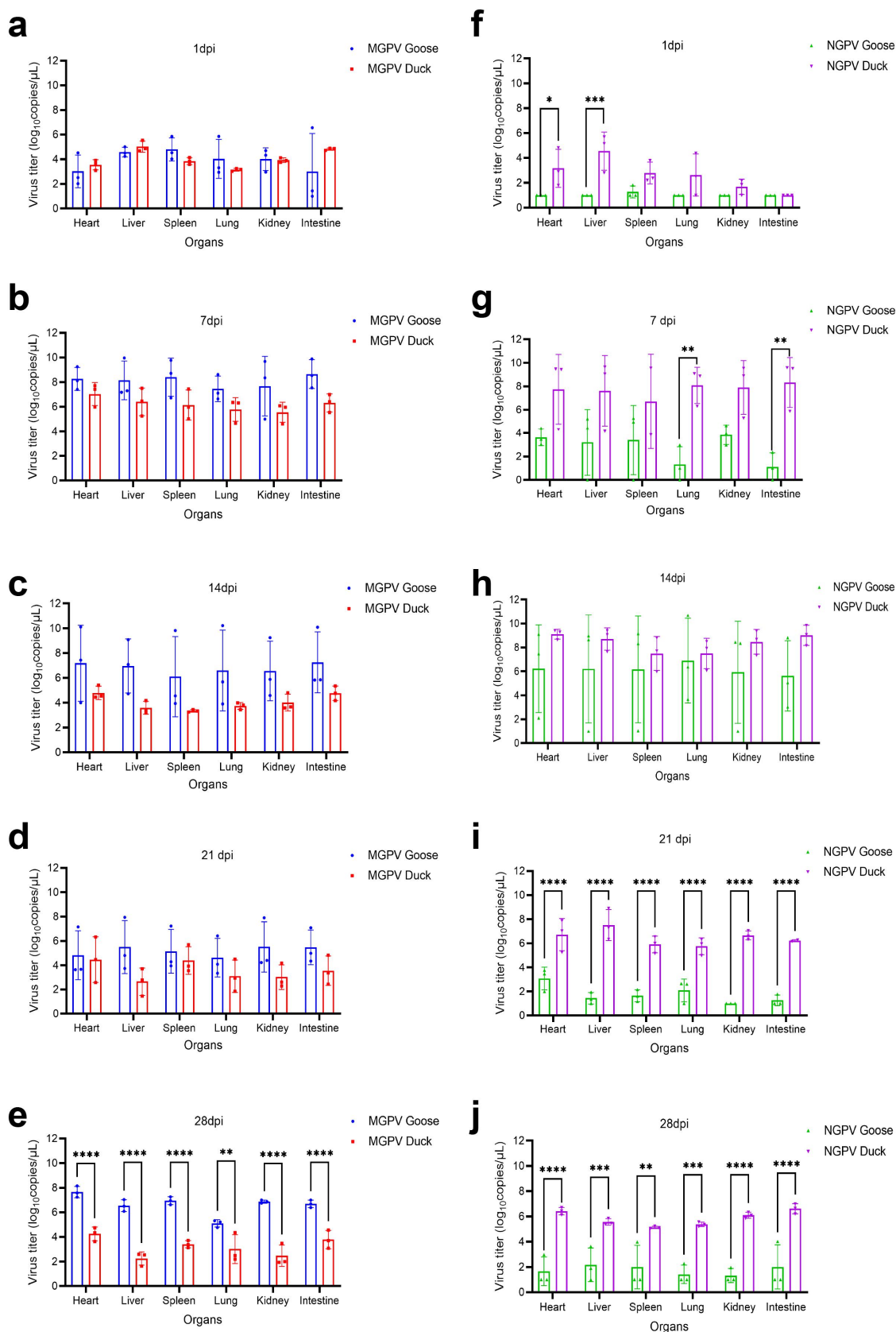


**Figure 7.** Viral load of organs from goslings/ducklings infected with MGPV and NGPV. Post-virus challenge, three unmarked animals per group were euthanized at 1, 7, 14, 21, and 28 dpi, and the heart, liver, spleen, lungs, kidneys, and intestines were collected aseptically. Viral load of (a–e) MGPV and (f–j) NGPV in each organ was assessed by qPCR following organ processing and DNA extracting. Virus replication levels and statistical analysis were generated using GraphPad prism 8.0. \* $p < 0.05$ , \*\* $p < 0.01$ , \*\*\* $p < 0.001$ , \*\*\*\* $p < 0.0001$ .



number in ducklings after 7 dpi (averaging  $\geq 10^{6.7}$  copies/ $\mu\text{L}$  of NGPV and  $\geq 10^{5.6}$  copies/ $\mu\text{L}$  of MGPV), with a significant difference in copy numbers across different organs at 28 dpi (averaging  $\geq 10^{5.1}$  copies/ $\mu\text{L}$  of NGPV and  $\geq 10^{2.5}$  copies/ $\mu\text{L}$  of MGPV) (Figure 8f,g,h,i,j). These findings suggest that MGPV replicates more robustly in goslings than NGPV, whereas NGPV demonstrates a stronger replication in ducklings than MGPV.

### **MGPV and NGPV induced differential humoral responses**

To evaluate the humoral responses of MGPV and NGPV, an indirect ELISA was used to quantify antibody titers in serum. Antibody levels against GPV in both infected groups increased over time, with MGPV eliciting higher titers than NGPV in goslings, a significant difference being observed from 21 dpi. Conversely, NGPV induced higher antibody levels than MGPV in ducklings ( $\text{OD}_{450}$  values: averaging  $\geq 0.2$  of NGPV and  $\geq 0.1$  of MGPV) (Figure 9). These findings indicate that MGPV and NGPV induce specific antibody production in goslings and ducklings, with MGPV demonstrating greater efficacy in goslings and NGPV in ducklings. Additionally

To evaluate the cross-reactivity between MGPV and NGPV, we used an indirect ELISA test. This test checks for reactions between specific viral antigens and antibodies. A P/N ratio of 2.1 or higher means a positive result; anything less is negative. The findings revealed that both MGPV and NGPV antigens could react with sera from their respective groups, suggesting some level of cross-reactivity between different GPV strains. MGPV showed a stronger response across various serum groups, with a minimum dilution of 1:8000 for both MGPV/anti-NGPV and anti-MGPV sera. In contrast, NGPV's reactivity topped out at a 1:500 dilution. Therefore, MGPV elicits a stronger humoral response than NGPV.

### **Discussion**

GPV is widely prevalent in goslings and ducklings, leading to an illness termed gosling plague. Interestingly, GPV is regarded as non-pathogenic to Cherry Valley and Peking ducks [21]. In 2015, a novel waterfowl parvovirus, genetically closely related to GPV, was isolated from a Cherry Valley duck flock. This virus induced SBDS in ducks and was classified as a new variant of GPV, named NGPV [8]. Epidemiological studies in recent years indicate that

NGPV is the predominant strain in ducks [22]. Extensive research has focused on elucidating the pathogenic characteristics of these isolates [23,24]. Concurrently, the isolate rate of MGPV in geese is rising, edging out the classical GPV, whereas its pathogenicity is less understood. To assess the comparative pathogenicity of the prevalent NGPV and MGPV in waterfowl, we conducted a systematic series of pathogenicity studies. It is well documented that the standard isolation method for GPV involves the use of goose and duck embryos, as well as the respective fibroblast cultures, allowing GPV replication both *in vitro* and in embryos [25–27]. In this study, we evaluated the infectivity of different GPV lineages on fibroblasts from geese and ducks. Our results indicate that both NGPV and MGPV strains can proliferate and induce cytopathic effects in these cells, corroborating the previous findings [28]. Furthermore, MGPV and NGPV can replicate within goose and duck embryos, respectively. These GPV strains showed an increasing replicative ability in the embryos, with viral titers rising as culture time extended, remaining low at 72 h and peaking between 144 to 192 h. Thus, when isolating GPV with goose and duck embryos, it is imperative to adjust the culture period to an appropriately extended duration. This contrasts with the culture times required for the isolation of other avian viruses, such as influenza virus [29], goose astrovirus [30], and duck novel reovirus [31]. The factors underlying these differences warrant further investigation.

Typically, viruses of distinct epidemic lineages may exhibit host-specific characteristics. For instance, H5 AIV is highly prone in waterfowl, with H5N2, H5N8, and H5N1 subtypes showing varied pathogenicity in ducks, but only H5N1 causing significant clinical symptoms and mortality [32]. NDV, known for its varied genotypes, is prevalent among waterfowl species [33]. Class I NDVs are largely harmless to poultry, in contrast to Class II NDVs that can cause disease and fatalities [34,35]. The pathogenicity of GPV across multiple epidemic strains has been investigated, yet a comprehensive comparative analysis of the pathogenic potential between NGPV and MGPV is still lacking [21,36,37]. This study revealed that the pathogenicity of MGPV and NGPV in goslings and ducklings displayed host-specific variability. Ducklings were usually more susceptible to NGPV infection, while goslings were more prone to MGPV infection. Despite recent epidemiological results indicating that NGPV isolates primarily originated from ducks, the infection studies suggest that NGPV poses an infection risk to geese. Antigenic variation among GPV strains has been previously documented [38]. To assess the antigenic



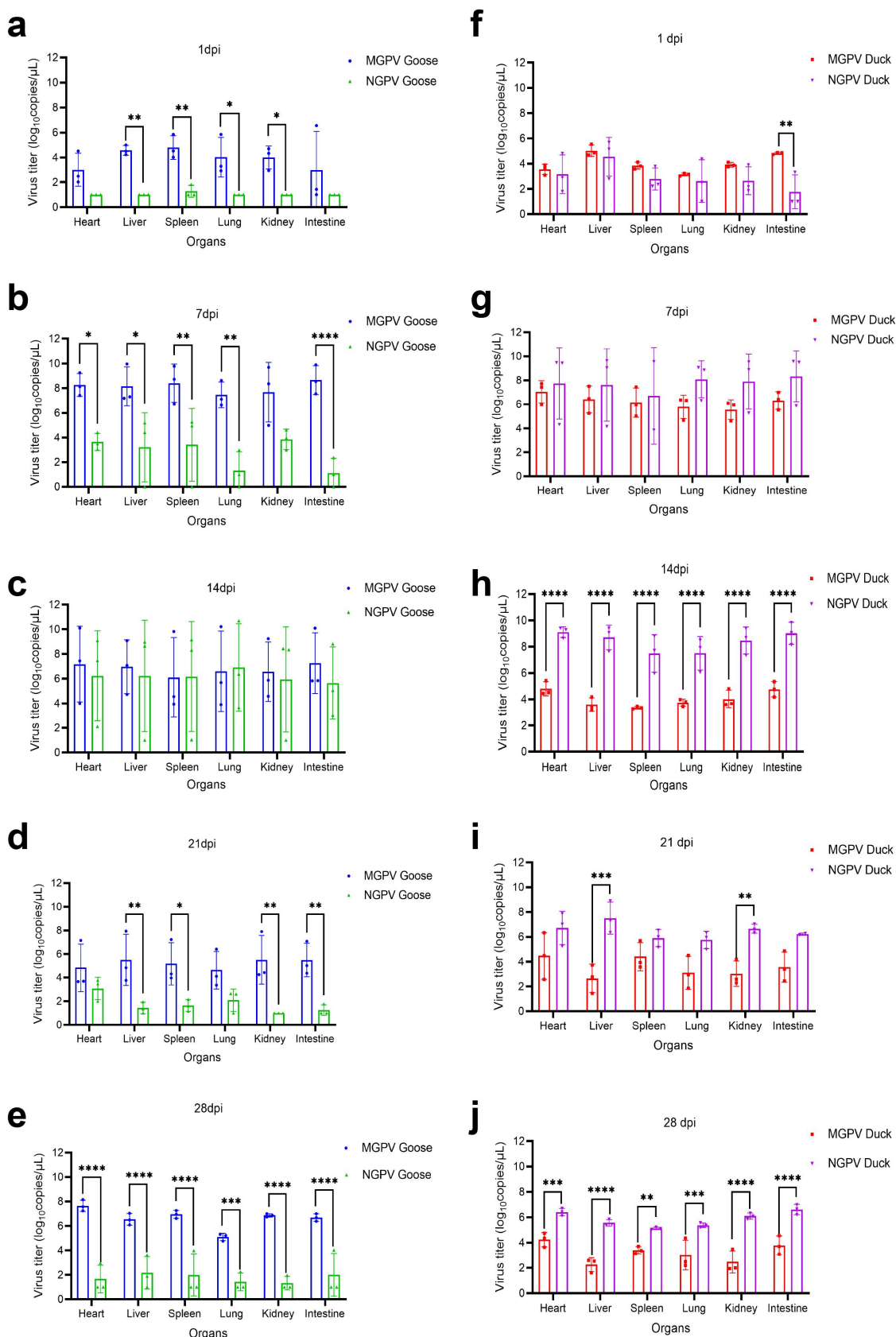


**Figure 8.** Comparative analysis of host susceptibility of MGPV and NGPV. Post-virus challenge, three unmarked animals per group were euthanized at 1, 7, 14, 21, and 28 dpi, and the heart, liver, spleen, lungs, kidneys, and intestines were collected aseptically. The viral loads of MGPV and NGPV across each organ in (a-e) goslings and (f-j) ducklings were subjected to comparative analysis, thereby evaluating the host susceptibility. Virus replication levels and statistical analysis were generated using GraphPad prism 8.0. \* $p < 0.05$ , \*\* $p < 0.01$ , \*\*\* $p < 0.001$ , \*\*\*\* $p < 0.0001$ .

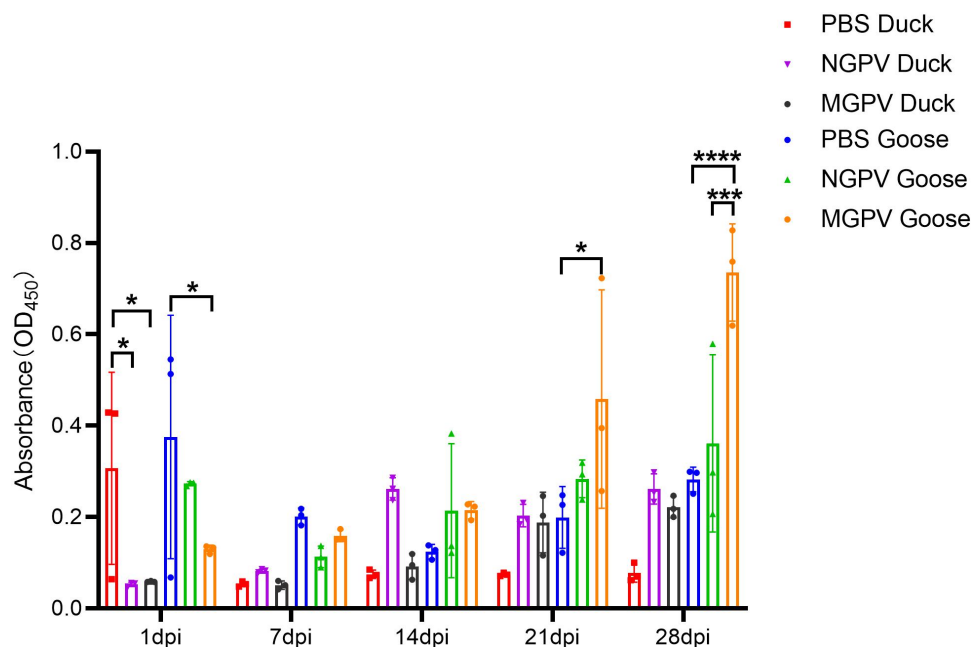


**Figure 9.** Detection of antibody levels in serum of goslings/ducklings infected with GPV. Following the virus challenge experiments, blood samples were drawn from each animal. The blood samples were processed, and antibody levels in the serum were quantified using an indirect ELISA. The optical density at 450 nm was recorded to determine antibody levels. \* $p < 0.05$ , \*\*\* $p < 0.001$ , \*\*\*\* $p < 0.0001$ .

difference between NGPV and MGPV, we quantified antibody responses in challenged animals. Following viral infection, the host immune system can mobilize to combat the virus, thereby resulting in the production of specific antibodies [39]. Here, NGPV and MGPV elicited higher antibody titers in ducklings and goslings, respectively, indicating potential host-specific immune responses of different GPV strains. However, antibody production is just one aspect of the host immune response. Future studies should delve into other immune system components, like cytokine regulation and T-cell proliferation, for a more comprehensive understanding. Additionally, cross-reactivity is observed among GPV strains, with MGPV demonstrating greater humoral response compared to NGPV. Differences in amino acids between MGPV and NGPV, especially in GPV's linear epitopes, likely explain the varying humoral response of these strains. The cross-reactivity is essential for the development of an effective vaccine, especially the wide spectrum viral vaccines [40]. Therefore, MGPV demonstrates robust cross-reactivity, suggesting promising potential for wide spectrum vaccine development.

NGPV is associated with the hallmark clinical feature of SBDS in ducklings, whereas MGPV typically elicits the classic symptoms of gosling plague [21,41]. This study demonstrated that NGPV was more effective at causing SBDS in ducklings than MGPV, indicating NGPV as the

main cause of SBDS. Conversely, MGPV infection triggered the characteristic symptoms and pathology of gosling plague. We used a range of imaging techniques to thoroughly assess skeletal growth after NGPV infection. The X-ray and Micro-CT imaging assays confirmed that NGPV infection compromised bone integrity in infected ducklings, increasing their susceptibility to osteoporosis and fractures. Histological examination revealed incomplete tibial development, marked by an abundance of chondrocytes and the absence of a formed marrow cavity. Therefore, NGPV infection can significantly impair the skeletal growth of ducklings. This study represents the pioneering application of advanced imaging techniques in GPV research.

In summary, NGPV and MGPV exhibit distinct pathogenic and immunogenic profiles in different waterfowl. NGPV preferentially targets ducklings, resulting in SBDS, while MGPV is more pathogenic in goslings, inducing the classic symptoms of gosling plague. Both MGPV and NGPV triggered a humoral response in the hosts, but MGPV caused a stronger humoral response compared to NGPV. These insights advance our knowledge of the pathogenicity of prevalent GPV strains in waterfowl, providing a vital theoretical basis for the development of strategies to prevent and control GPV.

## Disclosure statement

No potential conflict of interest was reported by the author(s).

## Funding

This study was funded by the National Key Research and Development Project of China [2023YFD1800601, 2023YFD1800605], the National Natural Science Foundation of China [32302840, 32302958, 32402852], the Open Project Program of Jiangsu Key Laboratory of Zoonosis [R1808], the Priority Academic Program Development of Jiangsu Higher Education Institutions [PAPD], the Earmarked Fund For China Agriculture Research System [CARS-40], and the 111 Project D18007. The funder played no role in study design, data collection, analysis and interpretation of data, or the writing of this manuscript.

## Author contributions

XLL conceptualized the manuscript and drafted the initial version. QXQ performed experiments. MC and MQL generated data. XQW was involved in study design and editing manuscript. YHW generated a key resource. WHY, KTL, and RYG contributed ideas. YC, JH, MG, and SLH commented on the text. XFL and XWL secured funding to generate a key reagent. All authors have read and approved the final manuscript.

## Statement of adherence to arrive guidelines

In this study, we followed the Animal Research: Reporting of In Vivo Experiments (ARRIVE) guidelines to ensure transparency and integrity in the design, execution, and reporting of our experiments. The ARRIVE guidelines are intended to improve the quality of scientific research, ensure that experimental animal use is properly justified, and to promote the reliability and reproducibility of scientific discoveries. We have adhered to ARRIVE guidelines and upload a completed checklist as supplementary files.

## Data availability statement

The raw sequence data of this study are openly available in Figshare at <https://doi.org/10.6084/m9.figshare.27063460>

## ORCID

Jiao Hu  <http://orcid.org/0000-0001-6894-4436>

Min Gu  <http://orcid.org/0000-0002-4670-9109>

Shunlin Hu  <http://orcid.org/0009-0004-0615-1253>

Xiufan Liu  <http://orcid.org/0000-0002-9924-6646>

Xiaowen Liu  <http://orcid.org/0009-0003-6802-5116>

## References

- [1] Zhu Z, Liu D, Wan C. Editorial: waterfowl production and management strategies: nutrition, genetics and breeding, and diseases prevention. *Front Vet Sci.* 2023 Jan 5;10:1352086. doi: [10.3389/fvets.2023.1352086](https://doi.org/10.3389/fvets.2023.1352086)
- [2] Hassan MSH, Abdul-Careem MF. Avian viruses that impact table egg production. *Animals.* 2020 Sep 25;10(10):1747. doi: [10.3390/ani10101747](https://doi.org/10.3390/ani10101747)
- [3] Zadori Z, Erdei J, Nagy J, et al. Characteristics of the genome of goose parvovirus. *Avian Pathol.* 1994 Jun 10;23(2):359–364. doi: [10.1080/03079459408419004](https://doi.org/10.1080/03079459408419004)
- [4] Chen S, Liu P, He Y, et al. The 164 K, 165 K and 167 K residues in 160YPVVKPKLTEE171 are required for the nuclear import of goose parvovirus VP1. *Virology.* 2018 Apr 06;519:17–22. doi: [10.1016/j.virol.2018.03.020](https://doi.org/10.1016/j.virol.2018.03.020)
- [5] Yuan K, Wang D, Luan Q, et al. Whole genome characterization and genetic evolution analysis of a new ostrich parvovirus. *Viruses.* 2020 Mar 19;12(3):334. doi: [10.3390/v12030334](https://doi.org/10.3390/v12030334)
- [6] Fan W, Sun Z, Shen T, et al. Analysis of evolutionary processes of species jump in waterfowl parvovirus. *Front Microbiol.* 2017 Mar 14;8:421. doi: [10.3389/fmicb.2017.00421](https://doi.org/10.3389/fmicb.2017.00421)
- [7] Ma H, Gao X, Fu J, et al. Development and evaluation of NanoPCR for the detection of goose parvovirus. *Vet Sci.* 2022 Aug 27;9(9):460. doi: [10.3390/vetsci9090460](https://doi.org/10.3390/vetsci9090460)
- [8] Chen H, Dou Y, Tang Y, et al. Isolation and genomic characterization of a duck-origin GPV-Related parvovirus from Cherry Valley Ducklings in China. *PLOS ONE.* 2015 Oct 14;10(10):e0140284. doi: [10.1371/journal.pone.0140284](https://doi.org/10.1371/journal.pone.0140284)
- [9] Woźniakowski G, Samorek-Salamonowicz E, Kozdruń W. Quantitative analysis of waterfowl parvoviruses in geese and muscovy ducks by real-time polymerase chain reaction: correlation between age, clinical symptoms and DNA copy number of waterfowl parvoviruses. *BMC Vet Res.* 2012 Mar 15;8(1):29. doi: [10.1186/1746-6148-8-29](https://doi.org/10.1186/1746-6148-8-29)
- [10] Glávits R, Zolnai A, Szabó É, et al. Comparative pathological studies on domestic geese (*Anser anser domestica*) and muscovy ducks (*Cairina moschata*) experimentally infected with parvovirus strains of goose and muscovy duck origin. *Acta Vet Hung.* 2005 Jul 22;53(1):73–89. doi: [10.1556/AVet.53.2005.1.8](https://doi.org/10.1556/AVet.53.2005.1.8)
- [11] Niu Y, Zhao L, Liu B, et al. Comparative genetic analysis and pathological characteristics of goose parvovirus isolated in Heilongjiang, China. *Virol J.* 2018 Feb 1;15(1):27. doi: [10.1186/s12985-018-0935-5](https://doi.org/10.1186/s12985-018-0935-5)
- [12] Chen S, Wang S, Cheng X, et al. Isolation and characterization of a distinct duck-origin goose parvovirus causing an outbreak of duckling short beak and dwarfism syndrome in China. *Arch Virol.* 2016 June 17;161(9):2407–2416. doi: [10.1007/s00705-016-2926-4](https://doi.org/10.1007/s00705-016-2926-4)
- [13] Huo X, Chen Y, Zhu J, et al. Evolution, genetic recombination, and phylogeography of goose parvovirus. *Comp Immunol Microbiol Infect Dis.* 2023 Oct 6;102:102079. doi: [10.1016/j.cimid.2023.102079](https://doi.org/10.1016/j.cimid.2023.102079)
- [14] He D, Wang F, Zhao L, et al. Epidemiological investigation of infectious diseases in geese on mainland China during 2018–2021. *Transbound Emerg Dis.* 2022 Feb 2;69(6):3419–3432. doi: [10.1111/tbed.14699](https://doi.org/10.1111/tbed.14699)
- [15] Zhan G, Liu N, Fan X, et al. Genome cloning and genetic evolution analysis of eight duck-sourced novel goose parvovirus strains in China in 2023. *Front Microbiol.* 2024 May 2;15:1373601. doi: [10.3389/fmicb.2024.1373601](https://doi.org/10.3389/fmicb.2024.1373601)
- [16] Soliman MA, Erfan AM, Samy M, et al. Detection of novel goose parvovirus disease associated with short beak and dwarfism syndrome in commercial ducks.

- Animals. 2020 Oct;10(10):1833. doi: [10.3390/ani10101833](https://doi.org/10.3390/ani10101833)
- [17] Wang J, Wang Y, Li Y, et al. Reproduction and pathogenesis of short beak and dwarfism syndrome in Cherry Valley Pekin ducks infected with the rescued novel goose parvovirus. *Virulence*. 2022 May 3;13(1):844–858. doi: [10.1080/21505594.2022.2071184](https://doi.org/10.1080/21505594.2022.2071184)
- [18] Ning K, Liang T, Wang M, et al. Pathogenicity of a variant goose parvovirus, from short beak and dwarfism syndrome of Pekin ducks, in goose embryos and goslings. *Avian Pathol*. 2018 Aug 24;47(4):391–399. doi: [10.1080/03079457.2018.1459040](https://doi.org/10.1080/03079457.2018.1459040)
- [19] Rayes J, Lax S, Wichaiyo S, et al. The podoplanin-CLEC-2 axis inhibits inflammation in sepsis. *Nat Commun*. 2017 Dec 21;8(1):2239. doi: [10.1038/s41467-017-02402-6](https://doi.org/10.1038/s41467-017-02402-6)
- [20] Ulici V, Hoenselaar KD, Agoston H, et al. The role of Akt1 in terminal stages of endochondral bone formation: angiogenesis and ossification. *Bone*. 2009 Aug 11;45(6):1133–1145. doi: [10.1016/j.bone.2009.08.003](https://doi.org/10.1016/j.bone.2009.08.003)
- [21] Ning K, Wang M, Qu S, et al. Pathogenicity of Pekin duck- and goose-origin parvoviruses in Pekin ducklings. *Vet Microbiol*. 2017 Sep 7;210:17–23. doi: [10.1016/j.vetmic.2017.08.020](https://doi.org/10.1016/j.vetmic.2017.08.020)
- [22] Li Y, Jia J, Mi Q, et al. Molecular characteristics and phylogenetic analysis of novel goose parvovirus strains associated with short beak and dwarfism syndrome. *Arch Virol*. 2021 Jul 7;166(9):2495–2504. doi: [10.1007/s00705-021-05145-4](https://doi.org/10.1007/s00705-021-05145-4)
- [23] Hoan TD, Thao DT, Huong Giang NT, et al. Molecular identification and pathogenicity of novel duck-origin goose parvovirus isolated from beak atrophy and dwarfism syndrome of Waterfowls in the north of Vietnam. *Avian Dis*. 2022 Sep 9;66(3):1–12. doi: [10.1637/aviandiseases-D-21-00087](https://doi.org/10.1637/aviandiseases-D-21-00087)
- [24] Zhu Y, Wu Q, Wu M, et al. Pathogenicity of duck circovirus and novel goose parvovirus co-infection in SPF ducks. *Avian Pathol*. 2024 Aug 22(1):1–7. doi: [10.1080/03079457.2024.2383231](https://doi.org/10.1080/03079457.2024.2383231)
- [25] Shao H, Jiang Y, Yuan H, et al. Generation and molecular characteristics of a highly attenuated GPV strain through adaptation in GEF cells. *BMC Vet Res*. 2020 Nov 23;16(1):456. doi: [10.1186/s12917-020-02673-0](https://doi.org/10.1186/s12917-020-02673-0)
- [26] Malkinson M, Winocour E. Adeno-associated virus type 2 enhances goose parvovirus replication in embryonated goose eggs. *Virology*. 2005 Jun 5;336(2):265–273. doi: [10.1016/j.virol.2005.03.019](https://doi.org/10.1016/j.virol.2005.03.019)
- [27] Yang YT, Deng ZC, Zhang LJ, et al. Novel goose parvovirus VP1 targets IRF7 protein to block the type I interferon upstream signaling pathway. *Poult Sci*. 2024 Jul 6;103(9):104065. doi: [10.1016/j.psj.2024.104065](https://doi.org/10.1016/j.psj.2024.104065)
- [28] Zhu J, Yang Y, Zhang X, et al. Characterizing two novel goose parvovirus with different origins. *Transbound Emerg Dis*. 2022 Sep 25;69(5):2952–2962. doi: [10.1111/tbed.14453](https://doi.org/10.1111/tbed.14453)
- [29] Eisfeld AJ, Neumann G, Kawaoka Y. Influenza a virus isolation, culture and identification. *Nat Protoc*. 2014 Oct 16;9(11):2663–2681. doi: [10.1038/nprot.2014.180](https://doi.org/10.1038/nprot.2014.180)
- [30] Wei F, He D, Wu B, et al. Isolation, identification, and pathogenicity of a goose astrovirus genotype 1 strain in goslings in China. *Viruses*. 2024 Mar 30;16(4):541. doi: [10.3390/v16040541](https://doi.org/10.3390/v16040541)
- [31] Huang C, Huang Y, Liu Z, et al. Isolation and characterization of a duck reovirus strain from mature ducks in China. *Poult Sci*. 2023 Nov 25;102(2):102345. doi: [10.1016/j.psj.2022.102345](https://doi.org/10.1016/j.psj.2022.102345)
- [32] Pantin-Jackwood MJ, Costa-Hurtado M, Shepherd E, et al. Pathogenicity and transmission of H5 and H7 highly pathogenic avian influenza viruses in mallards. *J Virol*. 2016 Nov 1;90(21):9967–9982. doi: [10.1128/jvi.01165-16](https://doi.org/10.1128/jvi.01165-16)
- [33] Alexander DJ. Gordon Memorial Lecture. Newcastle disease. *Br Poult Sci*. 2001 Jun 28;42(1):5–22. doi: [10.1080/713655022](https://doi.org/10.1080/713655022)
- [34] Lu X, Wang X, Zhan T, et al. Surveillance of class I Newcastle disease virus at live bird markets and commercial poultry farms in Eastern China reveals the epidemic characteristics. *Virol Sin*. 2021 Mar 15;36(4):818–822. doi: [10.1007/s12250-021-00357-z](https://doi.org/10.1007/s12250-021-00357-z)
- [35] Afonso CL. Virulence during Newcastle disease viruses cross species adaptation. *Viruses*. 2021 Jan 15;13(1):110. doi: [10.3390/v13010110](https://doi.org/10.3390/v13010110)
- [36] Yan Y-Q, He T-Q, Li R, et al. Molecular characterization and comparative pathogenicity of goose parvovirus isolated from Jilin province, Northeast China. *Avian Dis*. 2019 Sep 1;63(3):481–485. doi: [10.1637/aviandiseases-D-19-00075](https://doi.org/10.1637/aviandiseases-D-19-00075)
- [37] Liu H, Yang C, Liu M, et al. Pathological lesions in the immune organs of ducklings following experimental infection with goose parvovirus. *Res Vet Sci*. 2019 Jul;125(125):212–217. doi: [10.1016/j.rvsc.2019.06.002](https://doi.org/10.1016/j.rvsc.2019.06.002)
- [38] Yu K, Ma X, Sheng Z, et al. Identification of goose-origin parvovirus as a cause of newly emerging beak atrophy and dwarfism syndrome in ducklings. *J Clin Microbiol*. 2016 Jul 25;54(8):1999–2007. doi: [10.1128/jcm.03244-15](https://doi.org/10.1128/jcm.03244-15)
- [39] Zhang J, Zhang X, Liu J, et al. Serological detection of 2019-nCoV respond to the epidemic: a useful complement to nucleic acid testing. *Int Immunopharmacol*. 2020 Jul 30;88:106861. doi: [10.1016/j.intimp.2020.106861](https://doi.org/10.1016/j.intimp.2020.106861)
- [40] Vieira GF, Chies JA. Immunodominant viral peptides as determinants of cross-reactivity in the immune system—can we develop wide spectrum viral vaccines? *Med Hypotheses*. 2005 Jul 26;65(5):873–879. doi: [10.1016/j.mehy.2005.05.041](https://doi.org/10.1016/j.mehy.2005.05.041)
- [41] Matczuk AK, Chmielewska-Władyka M, Siedlecka M, et al. Short beak and dwarfism syndrome in ducks in Poland caused by novel goose parvovirus. *Animals*. 2020 Dec 15;10(12):2397. doi: [10.3390/ani10122397](https://doi.org/10.3390/ani10122397)